Carbohydrate Polymers 113 (2014) 515–524

Contents lists available at ScienceDirect

Carbohydrate Polymers

journal homepage: www.elsevier.com/locate/carbpol

Structural studies of arabinan-rich pectic polysaccharides from *Abies sibirica* L. Biological activity of pectins of *A. sibirica*

Evgeny G. Shakhmatov[a], Philip V. Toukach[b], Elena A. Michailowa[c], Elena N. Makarova[a,*]

[a] Institute of Chemistry, Komi Science Centre, The Urals Branch of the Russian Academy of Sciences, Pervomaiskaya str., 48, Syktyvkar 167982, Russia
[b] Zelinsky Institute of Organic Chemistry, Russian Academy of Sciences, Leninsky prospekt 47, Moscow 119991, Russia
[c] Institute of Physiology, Komi Science Centre, The Urals Branch of the Russian Academy of Sciences, Pervomaiskaya str., 50, Syktyvkar 167982, Russia

ARTICLE INFO

Article history:
Received 29 April 2014
Received in revised form 17 July 2014
Accepted 18 July 2014
Available online 29 July 2014

Keywords:
Abies sibirica
Pectin
Arabinan
Wood greenery
NMR spectroscopy
β-L-Ara*f*

ABSTRACT

Highly branched arabinan-rich pectic polysaccharides, containing 84% of arabinose, was extracted from wood greenery of *Abies sibirica* L. The structure of arabinan was studied by the 1D and 2D NMR spectroscopy. The macromolecule backbone was represented mainly by RG-I (molar ratio GalA:Rha ~ 1.3:1) patterns with high degree of rhamnose branching. Side chains were comprised of 1,5-linked α-L-Ara*f* residues (the major part of polymer mass), 1,3,5-di-*O*- and 1,2,3,5-tri-*O*-linked α-L-Ara*f* residues, confirming the presence of highly branched 1,5-α-L-arabinan. Although most L-Ara*f* were in α-anomeric form, minor terminal β-L-Ara*f*-(1 → ... was detected. 1,4-β-D-linked Gal*p* residues found in the side chains account for minor AG-I or 1,4-galactan, as compared to arabinan. A tentative structure was proposed.

Polysaccharides obtained from Siberian fir greenery were screened for biological activity. Galacturonan had a strongest stimulating effect on germination and growth rate of seeds, germs and roots of *Triticum aestivum*, *Avena sativa*, and *Secale cereale*.

1. Introduction

Arabinans are constituents of primary cell wall in a variety of plant seeds, fruits and roots, for example, in the seeds of *Cajanus cajan* (Swamy & Salimath, 1991), *Gleditsia triacanthos* (Navarro, Cerezo, & Stortz, 2002), seeds of *Opuntia ficus-indica* prickly pear fruits (Habibi, Mahrouz, & Vignon, 2005), *Caesalpinia bonduc* (Mandal et al., 2011), in almond (Dourado, Cardoso, Silva, Gama, & Coimbra, 2006), in sugar beet pulp (Simkovic, Uhliariková, Yadav, & Mendichi, 2010), and in sugar beet (Westphal et al., 2010), in quinoa (*Chenopodium quinoa*) seeds (Cordeiro et al., 2012), in olive pulp (Cardoso, Ferreira, Mafra, Silva, & Coimbra, 2007) and in the roots of *Echinacea pallida* (Thude & Classen, 2005).

In most cases they are contained in branched regions of pectin polysaccharides (Ovodov, 2009). Arabinans are branched molecules with a backbone of linear α-(1,5)-linked arabinose residues mono- or di-substituted by α-(1,2)-linked and/or α-(1,3)-linked arabinose side chains, which again may be further branched (Ridley, O'Neill, & Mohnen, 2001; Yapo, 2011).

Fine chemical structure and polyfunctional properties are still a matter of discussion, although structural features of pectin polysaccharides are well described in literature (Atmodjo, Hao, & Mohnen, 2013; Harholt, Suttangkakul, & Scheller, 2010; Yapo, 2011). Identification of linkage patterns in various regions of a pectin macromolecule aims at deep elucidation of fine pectin structure and, consequently, better comprehension of plant cell wall functioning at the molecular level (Yapo, 2011).

Abies sibirica L. (Siberian fir), a large evergreen conifer with high part of greenery, is one of the dominant species in European Russia, west and east Siberian taiga. It has been used for therapy and prophylaxis in official and folk medicine for ages. In the previous studies, we have obtained pectin fractions of abienans AS_W and AS_A from wood greenery of Siberian fir by sequential extraction by water and hydrochloric acid (pH 4). Linear region of abienan AS_A was found to consist of partially methyl-esterified 1,4-α-D-galatopyranosyluronan, while branched region had an RG-I pattern. Side carbohydrate chains of RG-I abienan AS_A were formed by 1,4-β-D-galactan fragments and branched 1,5-α-L-arabinan (Makarova, Patova, Shakhmatov, Kuznetsov, & Ovodov, 2013).

The main aim of the present study is the structural characterization of a sediment obtained by concentration of water extract of *A. sibirica* wood greenery. The biological activity of this polysaccharide was tested against other pectin polysaccharides of fir greenery in account for germination ability and germination rate of seeds, germs and roots of selected cultivars of *Triticum aestivum* L., *Avena sativa* L. and *Secale cereale* L.

* Corresponding author. Tel.: +7 8212 218477; fax: +7 8212 218477.
E-mail address: makarowa.elena-ma@yandex.ru (E.N. Makarova).

http://dx.doi.org/10.1016/j.carbpol.2014.07.037
0144-8617/

2. Materials and methods

2.1. Processing of plant raw material and isolation of polysaccharides

Wood greenery was collected in October 2012 near Syktyvkar (Komi Republik, Russia). The isolation was performed according to a procedure described earlier (Makarova et al., 2013).

The residual raw material (100 g) was treated with distilled water under continuous stirring at 75 °C during 2 h (Fig. 1) to give abienan AS_W (6.5 g). The remaining material was treated with dilute hydrochloric acid at pH 3.8–4.2 with continuous stirring and heating to 75 °C during 2 h to give abienan AS_A (1.9 g). Each sample was extracted three times with the same solvent. Extract was treated as described earlier (Makarova et al., 2013).

The extracts were concentrated, and produced dense white–gray sediments (Fig. 1), which were found to dissolve after sequential treatment by aqueous ammonia and aqueous hydrochloric acid, but not after separate treatment by any of these reagents. The obtained solutions were dialyzed against distilled water, centrifuged, concentrated and lyophilized to give polysaccharide fractions AS_WN (250 mg) and AS_AN (729 mg) (see Table 1).

Fraction AS_WN (45 mg) was dissolved in 1 ml of distilled water and further fractionated by gel-filtration chromatography on sephacryl S-300 column. Fractions corresponding to separate peaks were collected together, concentrated and lyophilized to give polysaccharide fraction AS_WN_1 (16.1 mg, peak I) and fraction AS_WN_2 (13.8 mg, peak II) (see Table 1).

2.2. General analytical methods

The uronic acid content was determined by reacting the material with 3,5-dimethylphenol in concentrated sulphuric acid (Usov, Bilan, & Klochkova, 1995) and measuring absorbance at 400 nm and 450 nm using D-galacturonic acid (Sigma–Aldrich) as reference. Protein concentration was calculated using the Bradford procedure (Bradford, 1976) with bovine serum albumin (BSA) as reference. The amount of methyl ester groups was determined as previously described (Wood & Siddiqui, 1971) at 412 nm using methanol as reference. The analysis was carried out without a preliminary hydrolysis of the polysaccharide. Each experiment was repeated three times.

Absorption spectra were measured on the Shimadzu UV-1700 (PharmaSpec) spectrophotometer. The specific optical rotations were determined on a Polatronic MHZ polarimeter. Solutions were concentrated on a rotary evaporator under low pressure at 40–45 °C, centrifuged at 5000–6000 rpm for 10–20 min, and lyophilized.

Molecular weights and polydispersities of the polysaccharide fractions were determined by HPLC as described by Makarova et al. (2013).

Gel filtration chromatography was carried out on a Sephacryl S-300 column (1.3 cm × 37 cm, a void volume of 12 ml, Sigma, USA). Distilled water was used as an eluent at flow rate of 0.3 ml/min, fractions volume was 3 ml. The carbohydrate content in fractions was determined using the phenol–sulphuric acid procedure (Smith's procedure) with photocolorimetry carried out at 480 nm (Dubois, Gilles, Hamilton, Rebers, & Smith, 1956).

NMR spectra were recorded using Bruker Avance II 300 MHz NMR instrument for 3–5% solutions of polysaccharides in D_2O (99.9% D) at 303 K and 328 K. Samples were freeze-dried from 99.9% D_2O and dissolved in it again. Chemical shifts were referenced to internal DSS (^1H and ^{13}C at 0.00 ppm). NMR signals were assigned using two-dimensional (2D) COSY, TOCSY, ROESY, $\{^1H,^{13}C\}$ HSQC, and $\{^1H,^{13}C\}$ HMBC experiments. 2D TOCSY spectra were recorded using the MLEV-17 mixing sequence with spin-lock time of 90 ms. 2D ROESY experiments were performed with a mixing time of 200 ms.

During the spectra assignment, the reference ^{13}C NMR data for the unsubstituted residues and glycosylation effects were taken from a CSDB Carbohydrate NMR simulation tool (Toukach & Ananikov, 2013). Literature and database ^{13}C NMR spectra referenced to TMS were normalized using a correction of +1.56 ppm.

The absolute configuration of arabinose was determined by GLC of the acetylated (*S*)-2-octyl glycoside (Leontein & Lonngren, 1993).

2.3. Monosaccharide analysis

Samples (3–5 mg) were hydrolysed with 2 M TFA (1 ml) containing *myo*-inositol (1 mg/ml) at 100 °C for 5 h. The mixture of neutral monosaccharides was converted to alditol acetates (York, Darvill, McNeil, Stevenson, & Albersheim, 1985) and identified by gas–liquid chromatography (GLC) on the Shimadzu GC-2010AF chromatograph equipped with a flame ionization detector, using a capillary column HP-1 (Agilent, 30 m × 0.25 mm × 0.25 mcm). Helium was used as a carrier gas. GLC of alditol acetates was carried out at temperature programmed from 175 °C (1 min) to 250 °C (2 min) at the rate of 3 °C/min. The content of monosaccharides as a percent of the total preparation mass was calculated from the peak areas using the coefficients of detector response. *Myo*-inositol was used as an internal standard.

2.4. Ion-exchange chromatography of polysaccharide AS_WN on DEAE-cellulose

Polysaccharide AS_WN (80 mg) was dissolved in 0.01 M NaCl (3 ml) and fractionated on a DEAE-cellulose Cl^--form column (34.5 cm × 2.2 cm). The fractions were eluted consecutively with 0.01, 0.1, 0.2 M NaCl at flow rate of 1 ml/min, then collected and analysed by Smith's procedure (Dubois et al., 1956). The fractions corresponding to separate peaks were combined, concentrated, dialysed and lyophilized. Three polysaccharide fractions were as follows: AS_WN-D_0 (eluted with 0.01 M NaCl, 22 mg), AS_WN-D_1 (eluted with 0.1 M NaCl, 31 mg), AS_WN-D_2 (eluted with 0.2 M NaCl, 11 mg).

2.5. Enzymatic hydrolysis of polysaccharide AS_WN_1

Polysaccharide AS_WN_1 (30 mg) was dissolved in water (10 ml), and the aqueous solution (0.2 ml) of exo- and endo-1,4-α-D-polygalacturonase (1 mg, activity >1 U/mg, EC 3.2.1.15; Fluka, Germany) was added. The mixture was incubated at 37 °C for 4 h. The 1,4-α-D-polygalacturonase was inactivated by boiling at 100 °C and removed by centrifugation. The obtained solution was concentrated, dialyzed using 3.5 kDa pores and lyophilized. The resulting carbohydrate fraction was dissolved in 1 ml of distilled water and separated by gel chromatography on sephacryl S-300 column. The main peak corresponded to a polysaccharide fraction AS_WN_1-F (19 mg).

2.6. Isolation of the HG domains

Pectin AS_W (0.2%, w/v) was hydrolyzed with 2 M TFA at 100 °C during 1.5 h. The acid-insoluble fraction was separated by centrifugation after cooling down. The precipitate was washed by 96% ethanol until no monosaccharides were detected in supernatant, dispersed in water and gradually added aqueous ammonia until complete dissolution, then dialyzed and lyophilized. The obtained polysaccharide fragment was dissolved in water and fractionated by gel chromatography on sephacryl S-300 column. The main peak (27.1% as compared to AS_W) corresponded to a polysaccharide fragment AS_WH while the minor peak was not studied.

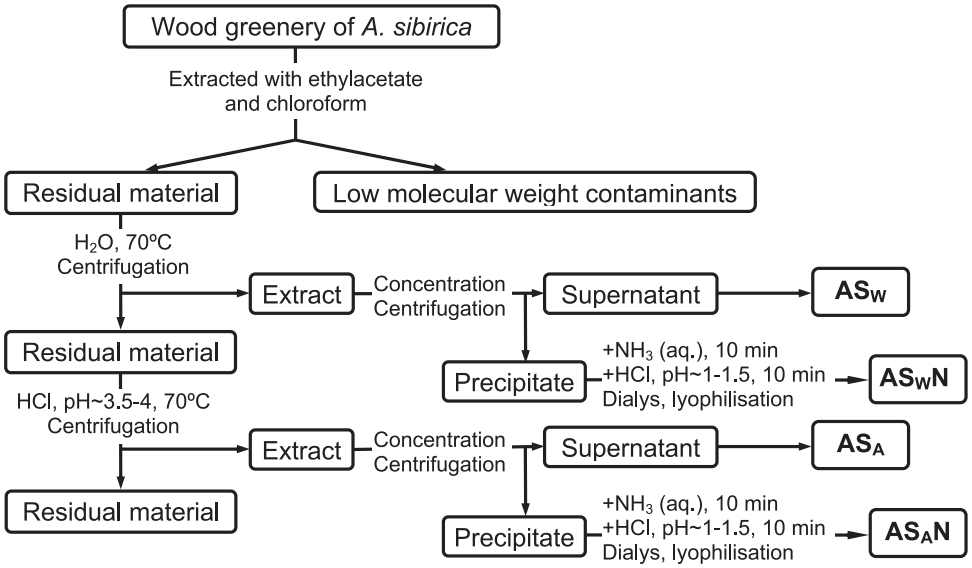

Fig. 1. The scheme of isolation of pectic polysaccharides from *Abies sibirica* L.

Table 1
Yields and composition (%, w/w) of polysaccharide fractions.

Fraction	Yield[a], %	$[\alpha]^{20}_D$	GalA	Neutral monosaccharides						Protein
				Gal	Ara	Rha	Xyl	Glc	Man	
AS_W	6.5	–	65.0	7.7	12.1	3.7	0.3	2.0	2.5	4.7
AS_WN	0.2	–	31.3	7.8	38.7	4.5	0.6	4.9	4.2	1.8
AS_WN_1	35.7[b]	+76	45.0	10.3	28.4	4.5	0.7	3.0	2.0	2.3
AS_WN_2	30.7[b]	+4.0	22.0	3.3	64.0	3.5	0.8	2.3	2.1	1.7
AS_WN-D_0	27.5[b]	−80	5.7	2.1	84.0	3.7	0.2	0.2	0.7	2.2
AS_WN-D_1	38.7[b]	+208	65.0	10.0	13.5	3.1	0.4	1.9	1.2	2.3
AS_WN-D_2	13.7[b]	+234	73.0	5.0	7.9	2.2	0.4	2.0	1.5	1.7
AS_WN_1-F	63.3[c]	–	34.5	12.8	32.4	7.1	1.0	3.7	2.9	2.1
AS_W-H	27.1[d]	+330	96.0	n.d.	n.d.	n.d.	n.d.	0.3	0.2	2.1
AS_A	1.9	–	55.0	13.2	17.0	5.2	0.7	2.4	2.0	3.8
AS_AN	0.7	–	54.5	8.0	14.6	5.7	0.6	2.4	3.9	0.7

n.d.–not detected.
[a] Polysaccharide yields are calculated from the air-dried plant material.
[b] Yield related to the quantity applied to the column.
[c] Yield, % of AS_WN_1.
[d] Yield, % of AS_W.

2.7. Biological activity of Siberian fir wood greenery polysaccharides

The effect of fir greenery polysaccharides on the early stage of cereal ontogenesis was studied using seeds of soft wheat (*T. aestivum* L.) cultivar "Irgina", oats (*A. sativa* L.) cultivar "Kirovskiy", and rye (*S. cereale* L.) cultivar "Falenskaya". Seeds were treated with 0.002% aqueous solutions of polysaccharides as described earlier (El'kina, Shubakov, & Ovodov, 2005) and controlled against seeds treated by tap water. The length of roots and aerial parts of cereals was measured on the 2nd, 4th, 6th and 8th day of germination of seeds and growth of germs. Germination and germinative energy were calculated in percent. The experiments were repeated four times, using 50 seeds in each experiment, and approved by a Student t-criterion. Statistical processing was performed in Microsoft Excel 97.

3. Results and discussion

3.1. Characterization of polysaccharides from Siberian fir

Plant cell wall hosts a series of interacting biochemical processes, such as biosynthesis, transformation and degradation of macromolecular components. These processes include depolymerization of polygalacturonan, cleavage of polysaccharide side chains, de-methyl-etherification of pectins, etc. (Gorshkova, 2007). Due to this, various metabolites of a pectin macromolecule are often extracted together with pectins themselves. Neutral polysaccharides present in cell wall in free form are known to have the structure more or less similar to that of RG-I side chains (Albersheim et al., 1996; Makarova et al., 2013).

Composition analysis and enzymatic hydrolysis of AS_WN and AS_AN polymers revealed characteristic components of RG-I: arabinose (38.7%, 14.6%), galactose (~8%), rhamnose (4.5%, 5.7%) and galacturonic acid (31.3%, 54.5%) (Table 1). Polymers AS_WN and AS_AN are most likely formed during biosynthesis and degradation of pectin and present in a cell wall as standalone polysaccharides.

Composition analysis of polysaccharide fractions AS_WN_1 and AS_WN_2 obtained by gel-filtration chromatography fractionation, revealed that they contained mainly GalA (up to 45%), Ara (up to 64%) and Gal (up to 10%) residues (Table 1). Mass characteristics of AS_WN_1 and AS_WN_2 determined by HPLC were *Mw* 59.0 and 11.7 kDa, and *Mw*/*Mn* 9.5 and 3.9, respectively.

3.2. Ion-exchange chromatography of polysaccharide AS_WN on DEAE-cellulose

Application of ion-exchange chromatography on DEAE-cellulose showed that polysaccharide fraction AS_WN contained

mainly neutral fraction $AS_WN\text{-}D_0$ (*Mw* 9.4 kDa) eluted by 0.01 M NaCl, presented by arabinan with ~84% of L-Ara and negative rotatory power, and two acidic fractions $AS_WN\text{-}D_1$ and $AS_WN\text{-}D_2$ eluted by 0.1 M and 0.2 M NaCl, respectively, with 65–73% of D-GalA and positive rotatory power (Table 1). Fraction $AS_WN\text{-}D_0$, were investigated thoroughly due to high content of arabinose.

Detection of GalA and Rha residues in $AS_WN\text{-}D_0$ implied presence of pectin polysaccharides (Table 1).

RG-I heteropolymer backbone is known to consist of 1,4-linked α-D-galacturonic acid residues and 1,2-linked partially substituted (at major at O4, at minor at O3) α-L-rhamnose residues. Gal*p*A:Rha ratio tends to be 1:1 or more (Atmodjo et al., 2013; Gorshkova, 2007).

RG-I content in pectins strongly depends on the biological source and extraction methods. For example, RG-I is a dominant (more than 50%) structural component in water-soluble pectin fractions from *Glycine max* (soybean) cotyledon and *Camellia sinensis* (green tea), and virtually the only structural component in the mucilage from *Abelmoschus esculentus* pod, *Linum usitatissimum* seed and *Arabidopsis thaliana* seed (Ele-Ekouna, Pau-Roblot, Courtois, & Courtois, 2011; Mikshina et al., 2012; Naran, Chen, & Carpita, 2008; Yapo, 2011).

The molar parts of HG and RG-I were calculated as follows: HG = GalA – Rha, RG-I = [GalA – HG] + Rha + Ara + Gal (Koffi, Yapo, & Besson, 2013; M'sakni et al., 2006). As judged by molar ratio HG:RG-I (1.1:97.9), a core of polysaccharide moiety in fraction $AS_WN\text{-}D_0$ is likely RG-I. Molar ratio GalA:Rha in fraction $AS_WN\text{-}D_0$ was calculated as 1.3:1.

This almost equimolar ratio is characteristic for RG-I, implying that fraction $AS_WN\text{-}D_0$ is built of repeating units [→4)-α-D-Gal*p*A-(1 → 2)-α-L-Rha*p*-(1→]. High Ara:Rha molar ratio of ~25 in $AS_WN\text{-}D_0$ assumes presence of arabinan in side chains of RG-I type (Caffall & Mohnen, 2009; Ridley et al., 2001). Arabinose residues in arabinans are typically in furanose form identified by high negative rotatory power in water solutions, but traces of arabinopyranoses have also been found (Steinhorn, Sims, Carnachan, Carr, & Schlothauer, 2011; Swamy & Salimath, 1991). The L-configuration of Ara was confirmed by GLC of the corresponding acetylated (S)-2-octyl glycosides (Makarova et al., 2013). Fraction $AS_WN\text{-}D_0$ was structurally characterized by the NMR spectroscopy.

High content of D-GalA (65–73%) and neutral monosaccharides (in major, arabinose, 10–13%; and galactose, 5–8%; see Table 1) showed that fractions $AS_WN\text{-}D_1$ and $AS_WN\text{-}D_2$ were mainly pectin polysaccharides (Table 1). Molar ratios GalA:Rha in the series $AS_WN\text{-}D_0$ (1.3:1) < $AS_WN\text{-}D_1$ (1.7:1) < $AS_WN\text{-}D_2$ (2.8:1) point to decreasing part of rhamnogalacturonan and growing part of homogalacturonan in this series.

3.3. NMR spectroscopy of polysaccharide $AS_WN\text{-}D_0$

^{13}C and ^{1}H NMR spectra were assigned using COSY, TOCSY, $^{1}H/^{13}C$ HSQC, ROESY and $^{1}H/^{13}C$ HMBC data (Figs. 2–4).

Low intensity signals in the HSQC spectrum of polysaccharide $AS_WN\text{-}D_0$ (Fig. 2) belong to D-Gal*p*A residues in a polysaccharide backbone. Their lower intensity can be explained by low α-D-Gal*p*A content (5.7%) and faster relaxation of their atoms as compared to less sterically affected arabinose residues in flexible side chains (Schols, Posthumus, & Voragen, 1990).

HMBC spectrum revealed signals of minor *O*-acetyl groups at δ 176.2/2.17–2.19 (not shown). It is known that backbone GalA in pectin polysaccharides can be acetylated at O-2 and/or O-3 positions, and the acetylation degree varies among biological sources (Perrone et al., 2002). Although we had no clear evidences of *O*-acetyl group attachment, we suggested that they partially acetylated 1,4-α-D-Gal*p*A residues. The ^{13}C NMR signals of the acetylated residues have not been resolved due to the low stoichiometric part of acetylation.

The HSQC spectrum upfield region contained C6/H6 signals at δ 19.0/1.30;1.24 from methyl groups of α-L-Rha*p* residues and C2/H2 correlations at δ 78.9/4.12 of 2-substituted α-L-Rha*p* residues. TOCSY spectrum of $AS_WN\text{-}D_0$ contained homonuclear correlations H2/H6 at δ 4.12/1.30, H3/H6 at δ 4.07/1.30, H2/H4 at δ 4.04/3.44, H2/H5/H6 at δ 4.04/3.78/1.24, H4/H6 at δ 3.44/1.24, which may belong to 1,2- and 1,2,4-linked α-L-Rha*p* residues (Table 2).

Chemical shifts of arabinose residues in the HSQC spectrum (Fig. 2, Table 2), as compared to the spectra of unsubstituted and various substituted α-L-Ara*f*, identified the presence of terminal, 1,5-linked, 1,3-linked, 1,3,5-linked and 1,2,3,5-linked α-L-Ara*f* in $AS_WN\text{-}D_0$ polysaccharide. Accordingly, COSY spectrum (Fig. 3) contained H1/H2, H2/H3, H3/H4, H4/H5;5′ correlations of these variously substituted α-L-Ara*f* residues (Table 2).

The COSY spectrum (Fig. 3) contained all vicinal correlations of 1,5-linked α-L-Ara*f* (A), which allowed full assignment of proton signals of this residue (H1 at δ 5.08, H2 4.12, H3 at δ 3.99, H4 at δ 4.21, H5;5′ at δ 3.86;3.80) close to that observed earlier (Makarova et al., 2013; Westphal et al., 2010). Corresponding carbon atoms (see Table 1) were assigned using HSQC data.

Protons (H2 at δ 4.36 and δ 4.38, and H3 at δ 3.96 and δ 3.95) of 1,3-linked α-L-Ara*f* residues C and D were assigned using vicinal cross-peaks in the COSY spectrum (Fig. 3), starting from H1 at δ 5.18 and 5.21, respectively. Ambiguities in the COSY spectrum were resolved basing on proton chemical shifts reported earlier (Cardoso et al., 2007; Nie et al., 2013; Redgwell et al., 2011). The assignment of the remaining protons in these spin system (H4 at δ 4.18, δ 4.23 and H-5;5′ at δ 3.87; δ 3.78) was done from TOCSY and ROESY data, and allowed carbon signal assignment via HSQC: δ 109.7, δ 82.1, δ 87.0, δ 84.7 δ 63.8 for C1-C5, respectively.

Signals of C1/H1 at δ 109.7/5.18 and C2/H2 at δ 89.7/4.16 in the HSQC spectrum (Fig. 2) were assigned to 1,2,5-linked α-L-Ara*f*. Due to low content of these residues, the remaining signals were not assigned. C2/H1 correlation at 89.7/5.18 in the HMBC spectrum (Fig. 4) confirmed 1–2 bond, and had chemical shifts reported for 1,2,5-linked α-L-Ara*f* (Mandal et al., 2011).

The HMBC spectrum (Fig. 4) contained *intra*-residue correlations of α-L-Ara*f* residues: C4/H1 (K) at δ 86.7/5.14, (L) at δ 86.7/5.17, (A) at δ 85.0/5.08, (B) at δ 84.1/5.11, (E) at δ 83.3/5.23; C3/H1 (K) at δ 79.3/5.14, (L) at δ 79.3/5.17, (A) at δ 79.5/5.08 (Table 2) (Cardoso et al., 2007; Cordeiro et al., 2012; Khodaei & Karboune, 2013; Shakhmatov, Toukach, Kuznetsov, & Makarova, 2014; Simkovic et al., 2010). Of *inter*-residue correlations, the HMBC spectrum contained C1(A)/H5;5′(A) (δ 110.2/3.86;3.80) and C5(A)/H1(A) (δ 69.5/5.08) correlations of residue A, identifying a fragment. . . → 5)-α-Ara*f*-(1 → 5)-α-Ara*f*-(1 → . . .. HMBC spectrum also contained C1(A)/H5;5′(E) and C3(E)/H1(A) correlations at 110.2/3.95;3.85 and δ 86.7/5.08, respectively, which matched 1,2,3,5-linked α-L-Ara*f* substitution by 1,5-linked α-L-Ara*f* at C5 characterized earlier (Habibi et al., 2005; Mandal et al., 2011; Westphal et al., 2010).

HMBC (Fig. 4) exhibited cross-peaks C1(K)/H2(E) at δ 109.7/4.30 (overlapping with other cross-peaks), C1(K)/H4(E) at δ 109.7/4.23, H1(K)/C4(E) at δ 5.14/83.3, C1(K)/H3(E) at δ 109.7/4.09, indicating a substitution of 1,2,3,5-linked α-L-Ara*f* by terminal α-L-Ara*f* at C2.

The ROESY spectrum contained *intra*- and *inter*-glycosidic cross-peaks H1/H3 at δ 5.08/3.99, H1/H5;5′ at δ 5.08/3.86;3.80 of α-L-Ara*f* residues. Observed NOEs of H1 with both H5 and H5′ confirmed a fragment. . . → 5)-α-Ara*f*-(1 → 5)-α-Ara*f*-(1 → . . .. Other observed NOEs were H1 of terminal α-L-Ara*f* with H3 of 1,3,5-linked or 1,2,3,5-linked α-L-Ara*f* at δ 5.17/4.08, which may account for substitution of residues (B) or (E) by terminal α-L-Ara*f* at C3;

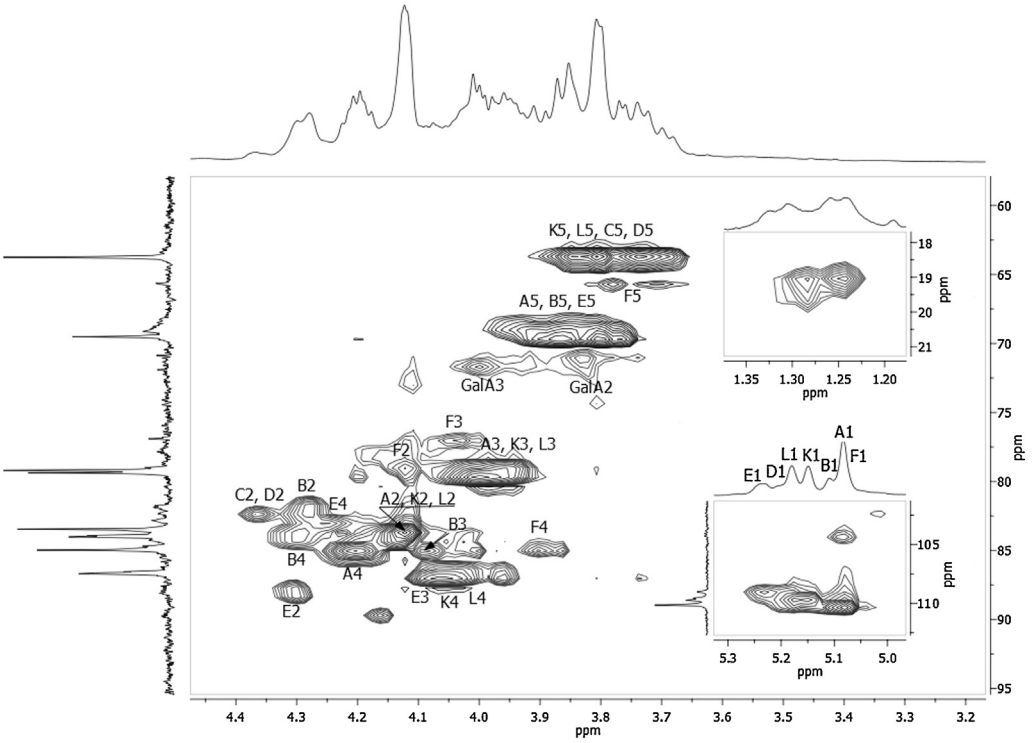

Fig. 2. $\{^{1}H,^{13}C\}$ HSQC spectrum of polysaccharide fragment $AS_WN\text{-}D_0$.

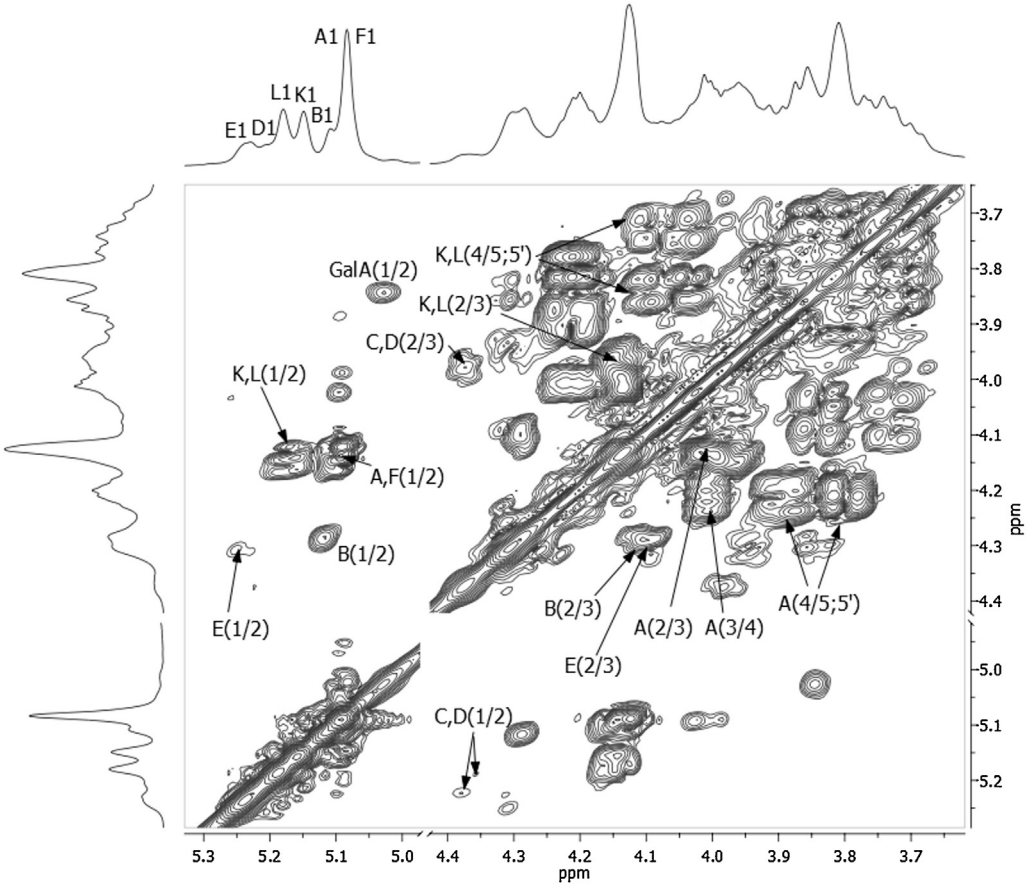

Fig. 3. COSY spectrum of polysaccharide fragment $AS_WN\text{-}D_0$.

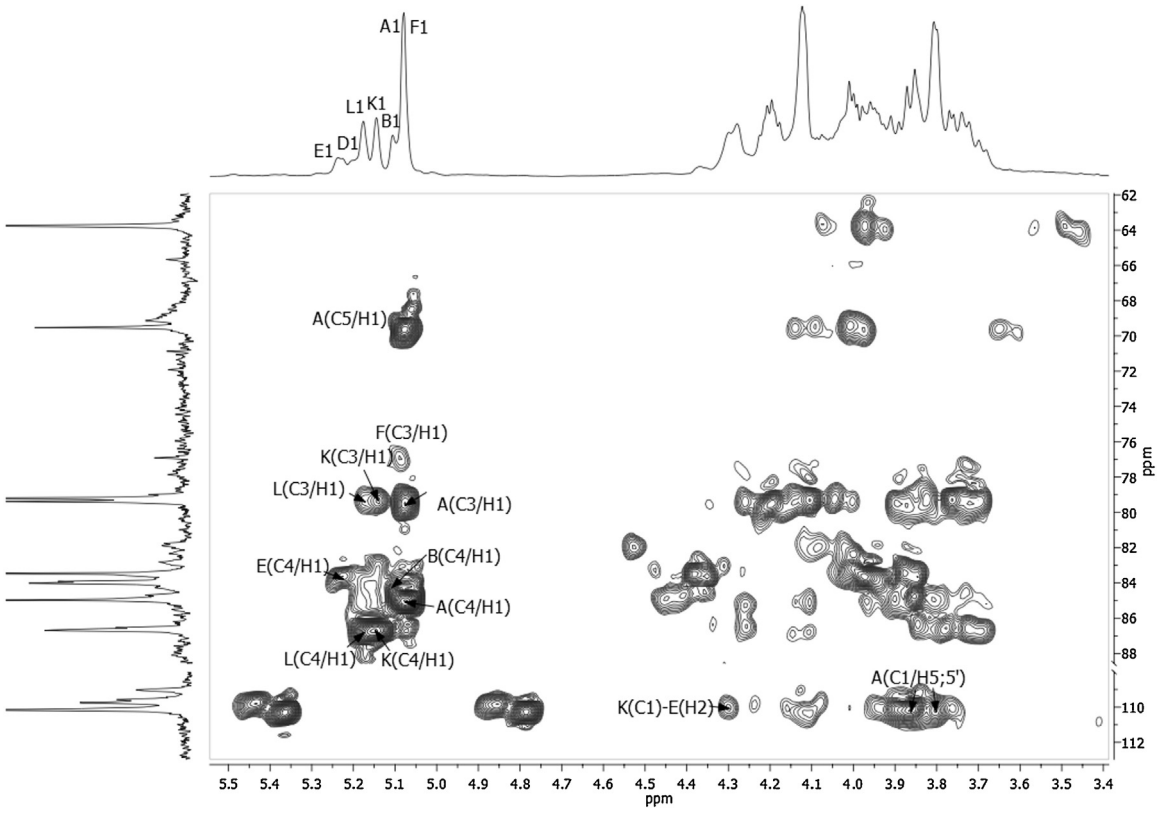

Fig. 4. Partial {^{1}H,^{13}C} HMBC spectrum of polysaccharide fragment AS$_{W}$N-D$_{0}$.

H1 α-L-Ara*f* (K)/H2 1,2,3,5-α-L-Ara*f* (E) at δ 5.14/4.30 м.д., confirming (1–2)-linkage between these residues; H1 1,2,3,5-α-L-Ara*f* (E)/H5,5′ 1,5-α-L-Ara*f* (A) at δ 5.23/3.86;3.80, which may arise from E(1–5)A fragment; and H1 1,3,5-α-L-Ara*f* (B)/H5,5′ 1,5-α-L-Ara*f* (A) at δ 5.11/3.86;3.80, which may arise from (1–5)-linkage between these residues.

Integral intensities of anomeric signals in the ^{1}H NMR spectrum of Ara*f* residues have a ratio (K + L):A:E:B:(C + D):G = 10.2:10.5:2.9:2.9:2.0:1.0. Thus terminal (∼34.5%) and 1,5-linked (∼35.6%) arabinose prevail over other linkage patterns of arabinose (1,3-, 1,3,5- 1,2,5- and 1,2,3,5-). High part of terminal and 1,2,3,5-linked (∼10.0%), 1,2,5-linked (3.4%) and 1,3,5-linked

Table 2
^{13}C and ^{1}H NMR data of polysaccharide fraction AS$_{W}$N-D$_{0}$, referenced to DSS.

Residue		C-1	C-2	C-3	C-4	C-5	C-6
		H-*1*	H-*2*	H-*3*	H-*4*	H-*5;5′*	H-*6;6′*
→4)-α-Gal*p*A-(1→		102.3[a] 5.02[a,b,d]	71.2[a] 3.82[a,b,d]	71.9[a] 3.99[a]	n.d.	n.d.	n.d.
→5)-α-Ara*f*-(1→	A	110.2[a,c] 5.08[a,b,c,d]	83.7[a] 4.12[a,b]	79.5[a,c] 3.99[a,b,d]	85.0[a,c] 4.21[a,b]	69.5[a,c] 3.86;3.80[a,b,c,d]	
→3,5)-α-Ara*f*-(1→	B	110.2[a] 5.11[a,b,c]	81.9[a] 4.28[a,b]	84.9[a] 4.08[a,b]	84.1[a,c] 4.31[a]	69.5[a] 3.95;3.85[a]	
→3)-α-Ara*f*-(1→	C	109.7[a] 5.18[a,b]	82.1[a] 4.36[a,b]	87.0[a] 3.96[a,b]	84.7[a] 4.23[a]	63.8[a] 3.87;3.78[a]	
→3)-α-Ara*f*-(1→	D	109.7[a] 5.21[a,b]	82.1[a] 4.38[a,b]	87.0[a] 3.95[a,b]	84.7[a] 4.18[a]	63.8[a] 3.87;3.78[a]	
→2,3,5)-α-Ara*f*-(1→	E	109.0[a] 5.23[a,b,c,d]	87.8[a] 4.30[a,b]	86.7[a] 4.09[a,b,d]	83.3[a,c] 4.23[a]	69.5[a] 3.95;3.85[a]	
→2,5)-α-Ara*f*-(1→	G	109.7[a] 5.18[a]	89.7[a] 4.16[a]	n.d.	n.d.	n.d.	
α-Ara*f*-(1→2	K	109.7[a] 5.14[a,b,c,d]	83.7[a] 4.13[a,b]	79.3[a,c] 3.96[a,b,d]	86.7[a,c] 4.05[a,b]	63.8[a] 3.83;3.73[a,b]	
α-Ara*f*-(1→3	L	109.7[a] 5.17[a,b,c,d]	83.8[a] 4.15[a,b]	79.3[a,c] 3.97[a,b,d]	86.7[a,c] 4.08[a,b]	63.8[a] 3.83;3.73[a,b]	
β-Ara*f*-(1→	F	104.3[a] 5.09[a,b,c]	79.0[a] 4.12[a,b]	77.0[a,c] 4.03[a]	85.0[a] 3.90[a]	65.7[a] 3.78;3.71[a]	
→4)-β-Gal*p*-(1→4		104.2[a] 4.63[b]	n.d. 3.69[b]	n.d. 3.76[d]	n.d. 4.16[d]	n.d. 3.75[d]	63.8[a] 3.78;3.72[a]

n.d.–not detected.
[a] Assignments from HSQC spectrum.
[b] Assignments from COSY spectrum.
[c] Assignments from HMBC spectrum.
[d] Assignments from ROESY spectrum.

(~9.8%) arabinose indicated a highly branched structure of arabinan. The backbone of the arabinan side-chain consisted of (1 → 5)-linked arabinose residues. The polymer repeating unit contained, on average, eleven unsubstituted residues, three residues substituted at O-3, three residues substituted at O-2 and O-3, and one residue substituted at O-2. Thus, Siberian fir arabinan possessed higher branching at O-3, than at O-2.

Branching at O-2 higher than at O-3, has been observed in arabinans from seeds of *C. cajan* (Swamy & Salimath, 1991) and *G. triacanthos* (Navarro et al., 2002), seeds of *O. ficus-indica* prickly pear fruits (Habibi et al., 2005) and *C. bonduc* (Mandal et al., 2011). On the contrary, arabinans branched mainly at O-3, as compared to O-2, were observed in almond (Dourado et al., 2006), in sugar beet pulp (Simkovic et al., 2010), and in sugar beet (Westphal et al., 2010). Arabinans from quinoa (*C. quinoa*) seeds, from Olive Pulp and from the roots of *E. pallida* had (1–5)-linked a-L-arabinofuranosyl units substituted exclusively at O-3 (Cardoso et al., 2007; Cordeiro et al., 2012; Thude & Classen, 2005).

High part of terminal α-L-Ara*f* (34.5%) and 6.7% of 1,3-linked α-L-Ara*f*, allow a suggestion that 1,5-linked α-L-Ara*f* side chains are either (1 → 3)-linked arabinose disaccharide or a single arabinose residue.

Although most L-Ara*f* had α-anomeric configuration, β-L-Ara*f* residues were found at side chain non-reducing ends. Their signals in the HSQC spectrum (C1/H1 at δ 104.3/5.09, C2/H2 at δ 79.0/4.12, C3/H3 at δ 77.0/4.03, C4/H4 at δ 85.0/3.90, C5/H-5;5′ at δ 65.7/3.78;3.71) were close to those reported for terminal β-Ara*f*-(1→ (Cardoso et al., 2007). Characteristic chemical shift of C2 (δ 79.0) revealed β-anomeric configuration of this residue. Assignment of C3 was confirmed by HMBC correlation at C3(F)/H1(F) δ 77.0/5.09.

Terminal β-Ara*f* residues were found in the arabinan from olive pectic polysaccharides. This structure was characterized by terminal β-Ara*f*, (1 → 5)-linked to (1 → 3,5)-Ara*f* residues and by the occurrence of branched and linear blocks in the arabinan backbone (Cardoso et al., 2007; Coimbra, Cardoso, & Lopes-da-Silva, 2010). As we know, the occurrence of β-Ara*f* in the arabinan pectic polysaccharides has only been credibly characterized by full NMR signal assignment for the olive pulp cell walls (Cardoso et al., 2007). Kim and Ralph examined loblolly pine (*Pinus taeda*, a gymnosperm) and aspen (*Populus tremuloides*, an angiosperm) and showed that the former had HSQC correlations in the anomeric region preliminary identified as belonging to β-L-Ara*f*, while the latter did not contain these residues (Kim & Ralph, 2010). Accordingly to our (Makarova & Shakhmatov) unpublished data, terminal β-Ara*f* residues are also present in polysaccharides from wood greenery of spruce.

Water-soluble acidic arabinogalactans from Norway spruce and Scots pine heartwood were analyzed and compared to Siberian larch heartwood (Willfor, Sjoholm, Laine, & Holmbom, 2002). Pine and larch AG samples displayed weak signals at δ 64.1–64.6 assigned to β-L-Ara*p* residues.

Besides *intra*-residue H1/H3 correlation at δ 4.63/3.76, confirming its β-anomeric configuration, β-Gal*p* residues exhibit a transglycosidic correlation H1/H4 in ROESY at δ 4.63/4.16, accounting for a. . . → 4)-β-Gal*p*-(1 → 4)-β-Gal*p*-(1 → . . . fragment (Makarova et al., 2013; Mikshina et al., 2012).

The AG-I backbone is known to consist of β-1,4-linked galactopyranose residues, substituted by terminal or monosubstituted α-L-Ara*f* residues at positions 2-O, 3-O (most often) or/and 6-O. The arabinan side chains are typically shorter, containing one to three Ara*f* residues. Nevertheless, arabinan side chains of up to 25 residues have been isolated from apple HR arabinogalactans by digestion with endo-(1 → 4)-β-D-galactanase (Endo-G) (Yapo, 2011).

We could not localize arabinose attachment to backbone due to low content of galactose branching points. Nevertheless, 1,4-linked β-D-Gal*p* observed together with α-L-Ara*f* residues allows a suggestion of AG-I presence in fraction $AS_WN\text{-}D_0$.

Arabinans, galactans and arabinogalactans varying from one to more than 50 residues in length can be attached to 20–80% of rhamnose residues (Gorshkova, 2007; Ridley et al., 2001). We suggest that side chains of RG-I are comprised of a branched arabinan; however, covalent linkage between arabinose and rhamnose residues has not been proved.

Integral intensities of rhamnose H6 signals in the ^{1}H NMR spectrum showed a ratio 1,2-α-L-Rha*p*: 1,2,4-α-L-Rha*p* as 50:50.

Mass content of 1,2,4-linked Rha*p* was calculated as ~1.85% of polysaccharide weight (3.7% w/w × 0.5). Mass content of 1,5-α-L-Ara*f* was calculated as 29% (84% w/w × 0.35). Thus, molar ratio of 1,5-α-L-Ara*f* to 1,2,4-α-L-Rha*p* is 19.3:1.13. It allows a suggestion that average length of oligomeric 1,5-α-L-Ara*f* chains is ~17 monomers, assumed that Ara*f* is attached to every residue of 1,2,4-linked α-L-Rha*p*. The average length of arabinan core including (1,5-α-L-Ara*f*, 1,3,5-α-L-Ara*f*, 1,2,5-α-L-Ara*f*, 1,2,3,5-α-L-Ara*f* residues) was calculated analogously as ~29 monomers.

According to monomeric composition analysis and NMR data, side chains of $AS_WN\text{-}D_0$ polysaccharide contain. . . → 4)-β-Gal*p*-(1 → 4)-β-Gal*p*-(1 → . . . fragment, which can substitute a part of 1,2,4-linked α-L-Rha*p*. Thus, arabinan core chains may be longer than 29 monomers as well. The length and branching degree of arabinan side chains depend on plant species and extraction method, and vary from 2 to 20 arabinose residues in sycamore to 45–118 arabinose residues in arabinans autoclavolytically released from sugar-beet pulp (Lerouge, O'Neill, Darvill, & Albersheim, 1993; Oosterveld, Beldman, Schols, & Voragen, 2000; Yapo, 2011).

Studied polysaccharides share characteristic structural features with pectic polysaccharides, extracted from wood greenery of *A. sibirica* by aqueous HCl (AS_A) earlier (Makarova et al., 2013). They have side chains of the similar structure, presented mainly by highly branched 1,5-α-L-arabinan fragments. Interpretation of the chemical shifts of the studied pectin AS_W-N simplified structural elucidation of the major fractions AS_W (unpublished data) and AS_A, as their NMR spectra expose complex overlaps and were not informative enough for complete structure elucidation. Particularly, signals of β-L-Ara*f* residues resolved in the present study, could not be interpreted in the previous study due to their low intensity.

3.4. Enzymatic hydrolysis of AS_WN_1 fragments

Enzymatic hydrolysis of AS_WN_1 polysaccharide by α-1,4-D-polygalacturonase followed by lysate fractionation by gel chromatography on sephacryl S-300 gave AS_WN_1-F fragment, corresponding to the biggest chromatographic peak (*Mw* 9.5 kDa). Its major carbohydrate components were GalA (34.5%), Ara (32.4%), Gal (12.8%) and Rha (7.1%) residues (Table 1).

Enzymatic hydrolysis of AS_WN_1 polysaccharide led to backbone cleavage and yielded free galacturonic acid. On the other hand, a product of enzymatic digestion, AS_WN_1-F had higher content of neutral monosaccharide residues and lower content of GalA, as compared to the source AS_WN_1 (see Table 1). These data together indicate presence of both branched regions (RG-I) and α-1,4-D-galacturonan in AS_WN_1.

3.5. NMR spectroscopy of polysaccharide AS_WN_1-F

In general, 1D and 2D NMR spectra of fraction AS_WN_1-F were similar to those of $AS_WN\text{-}D_0$, but had a few differences. Particularly, they revealed side chain regions rich in methyl-esterified 1,4-α-D-Gal*p*A residues (methylation degree was 59.7%) possessing the following resonances: C1/H1 at δ 102.2/5.03, C2/H2 at δ 71.6/3.83,

Table 3
Effect of polysaccharide fractions on growth rate of *T. aestivum* L. germs (2–8 days).

Fraction	Germination (%)				Germinative energy (%)		Root length (mm)				Germ length (mm)			
	2 days	4 days	6 days	8 days	2 days	8 days	2 days	4 days	6 days	8 days	2 days	4 days	6 days	8 days
Reference	42	49	58	72	17	51	6 ± 4	15 ± 5	22 ± 6	36 ± 10	–	9 ± 3	15 ± 5	27 ± 8
AS_W	44	50	61	79	21	64	7 ± 3	15 ± 4	26 ± 5	42 ± 7	–	12 ± 3	19 ± 4	35 ± 8
AS_WN	39	47	56	77	17	63	7 ± 5	16 ± 5	22 ± 4	38 ± 8	–	12 ± 4	13 ± 4	27 ± 6
AS_A	43	51	60	74	22	59	6 ± 3	17 ± 4	25 ± 5	38 ± 8	–	12 ± 3	17 ± 4	29 ± 7
AS_AN	33	42	57	78	14	65	5 ± 2	18 ± 4	24 ± 6	40 ± 7	–	5 ± 3	15 ± 6	30 ± 8
AS_W-H	60	66	72	88	28	81	12 ± 5	37 ± 7	48 ± 9	64 ± 12	4 ± 3	25 ± 7	39 ± 7	42 ± 11

Table 4
Effect of polysaccharide fractions on growth rate of *Avena sativa* L. germs (2–8 days).

Reference	Germination (%)				Germinative energy (%)		Root length (mm)				Germ length (mm)			
	2 days	4 days	6 days	8 days	2 days	8 days	2 days	4 days	6 days	8 days	2 days	4 days	6 days	8 days
Reference	–	24	35	58	6	36	–	8 ± 3	21 ± 5	36 ± 8	–	–	8 ± 5	15 ± 5
ASW	–	25	38	64	7	43	–	14 ± 6	25 ± 7	42 ± 7	–	–	15 ± 7	25 ± 8
ASWN	–	22	36	58	8	39	–	16 ± 7	22 ± 6	38 ± 8	–	–	9 ± 4	18 ± 5
ASA	–	27	36	60	7	38	–	14 ± 5	25 ± 5	38 ± 8	–	–	18 ± 7	18 ± 5
ASAN	–	20	38	62	8	44	–	16 ± 5	25 ± 5	30 ± 8	–	–	8 ± 4	20 ± 9
ASW-H	9	39	56	82	22	65	5 ± 4	28 ± 5	50 ± 7	58 ± 7	–	12 ± 4	25 ± 7	39 ± 9

Table 5
Effect of polysaccharide fractions on growth rate of *Secale cereale* L. germs (2–8 days).

Reference	Germination (%)				Germinative energy (%)		Root length (mm)				Germ length (mm)			
	2 days	4 days	6 days	8 days	2 days	8 days	2 days	4 days	6 days	8 days	2 days	4 days	6 days	8 days
Reference	48	52	62	68	19	52	7 ± 4	11 ± 5	28 ± 6	38 ± 8	–	7 ± 4	14 ± 4	21 ± 5
AS_W	49	56	65	73	23	56	10 ± 4	23 ± 6	34 ± 8	42 ± 7	–	11 ± 4	17 ± 4	28 ± 5
AS_WN	49	56	63	70	19	54	9 ± 3	23 ± 4	32 ± 8	38 ± 8	–	10 ± 4	16 ± 9	23 ± 5
AS_A	51	55	64	71	24	55	9 ± 4	18 ± 4	29 ± 7	39 ± 8	–	8 ± 5	16 ± 6	28 ± 5
AS_AN	53	57	65	67	22	52	10 ± 4	18 ± 5	35 ± 5	40 ± 10	–	9 ± 3	15 ± 10	22 ± 5
AS_W-H	62	69	78	86	35	74	16 ± 5	38 ± 5	50 ± 8	65 ± 7	4 ± 3	22 ± 7	35 ± 5	44 ± 7

C3/H3 at δ 71.7/4.01, C4/H4 at δ 81.9/4.46, C5/H5 at δ 73.6/5.16, C6 at δ 173.6 (Perrone et al., 2002; Petersen, Meier, Duus, & Clausen, 2008; Taboada et al., 2010; Zheng & Mort, 2008). Linkage of CH_3O— group (δ 55.8/3.81) to esterified carboxy carbon of GalA was proven by the HMBC correlation CH_3/C6 at δ 173.6/3.81 (see Supplemental Table 1 online).

Comparison of the spectra of different fractions indicated that significant part of α-1,4-D-galactopyranosyluronan of AS_WN_1-F bears methyl groups at Gal*p*A position C6.

It was concluded that carbohydrate moiety of AS_WN_1-F contained partially (DA 14%) acetylated 1,4-α-D-Gal*p*A. Signal of the acetyl group was observed in the HSQC spectrum at δ 23.1/2.16.

The HSQC spectrum contained rhamnose C6/H6 signals at δ 19.5/1.25;1.30. Comparative studies of COSY, TOCSY, ROESY and HSQC spectra of AS_WN-D_0 and AS_WN_1-F fractions revealed intensive signals of 1,2-, 1,2,4-linked α-L-Rha*p*, terminal, 1,5-, 1,3-, 1,3,5- and 1,2,3,5-linked α-L-Ara*f*, close to those in AS_WN-D_0 NMR spectra. This data account for the presence of branched 1,5-α-L-arabinan in AS_WN_1-F polysaccharide.

Low intensity signals in AS_WN_1-F were assigned to terminal, 1,3-linked, and 1,3,6-linked β-D-Gal*p*, as described earlier (Makarova et al., 2013).

3.6. Biological activity of fir greenery polysaccharides

The Pectic polysaccharides AS_W, AS_A, AS_WN, AS_AN and galacturonan AS_W-H were probed against their effect on germination ability and germination rate of seeds, and growth of germs and roots of soft wheat *T. aestivum* L., oats *A. sativa* L., and rye *Secale cereale L.*

Molar ratios of GalA to Rha were 15:1, 9.0:1, 8.9:1, and 6.0:1 in polysaccharides AS_W, AS_AN, AS_A, and AS_WN, respectively. Galacturonan AS_W-H was characterized by high content of GalA residues (96%) (Table 1). Thus, GalA:Rha ratio increased like AS_W-H > AS_W > AS_AN > AS_A > AS_WN, indicating growing part of HG and decreasing part of RG-I in this series. Compositional and structural studies distinguished polysaccharides by structural features caused by different length of HG and/or RG-I.

The biological activity measurement data (Tables 3–5) showed that all polysaccharides except galacturonan did not have a valuable effect on germination and growth of tested cultivars. On the contrary, galacturonan exhibited a significant growth-stimulatory effect. As compared to reference, cultivars from seeds treated by galacturonan solutions displayed the following behavior: germination ability increased by 22–31%, germination rate grew approx. twice, and root growth rate increased approx. by 60%.

Germinative energy was calculated from amount, weight and length of germs. All tested polysaccharides positively affected the germinative energy. Its increase was measured as 40–80% in the case of galacturonan compared to reference.

Thus, the maximal growth-stimulatory effect on germination and growth of germs and roots of *T. aestivum* L., *A. sativa* L., and *Secale cereale* L. belonged to a polysaccharide built of a linear α-1,4-D-galactopyranosyluronan backbone only.

4. Conclusions

The structural studies evidence for the presence of arabinan-rich pectic polysaccharides in Siberian fir wood greenery. Almost

equimolar ratio GalA:Rha (1.3:1) in fraction $AS_WN\text{-}D_0$ is characteristic for RG-I, and reveals a characteristic structural pattern of its backbone: [→4)-α-D-Gal*p*A-(1 → 2)-α-L-Rha*p*-(1→]. The backbone of $AS_WN\text{-}D_0$ polysaccharide consists mainly of RG-I regions with high content of rhamnose residues (~50%) at branching points. The attached side chains contain 1,5-α-L-Ara*f*, 1,3,5-Ara*f*, and 1,2,3,5 α-L-Ara*f* within a highly branched major 1,5-α-L-arabinan, and 1,4-β-D-Gal*p* within minor moiety of AG-I or 1,4-galactan. β-L-Ara*f* residues were found at non-reducing ends of side chains, which have not been reported for Siberian fir elsewhere.

Of fir greenery polysaccharides, galacturonan was shown to have maximal stimulatory effect on germination ability and rate of seeds, and growth of germs and roots of soft wheat (*T. aestivum* L.) cultivar "Irgina", oats (*A. sativa* L.) cultivar "Kirovskiy", and rye (*Secale cereale* L.) cultivar "Falenskaya".

The schematic structure of the arabinan-rich pectic polysaccharides can be summarized as follows:

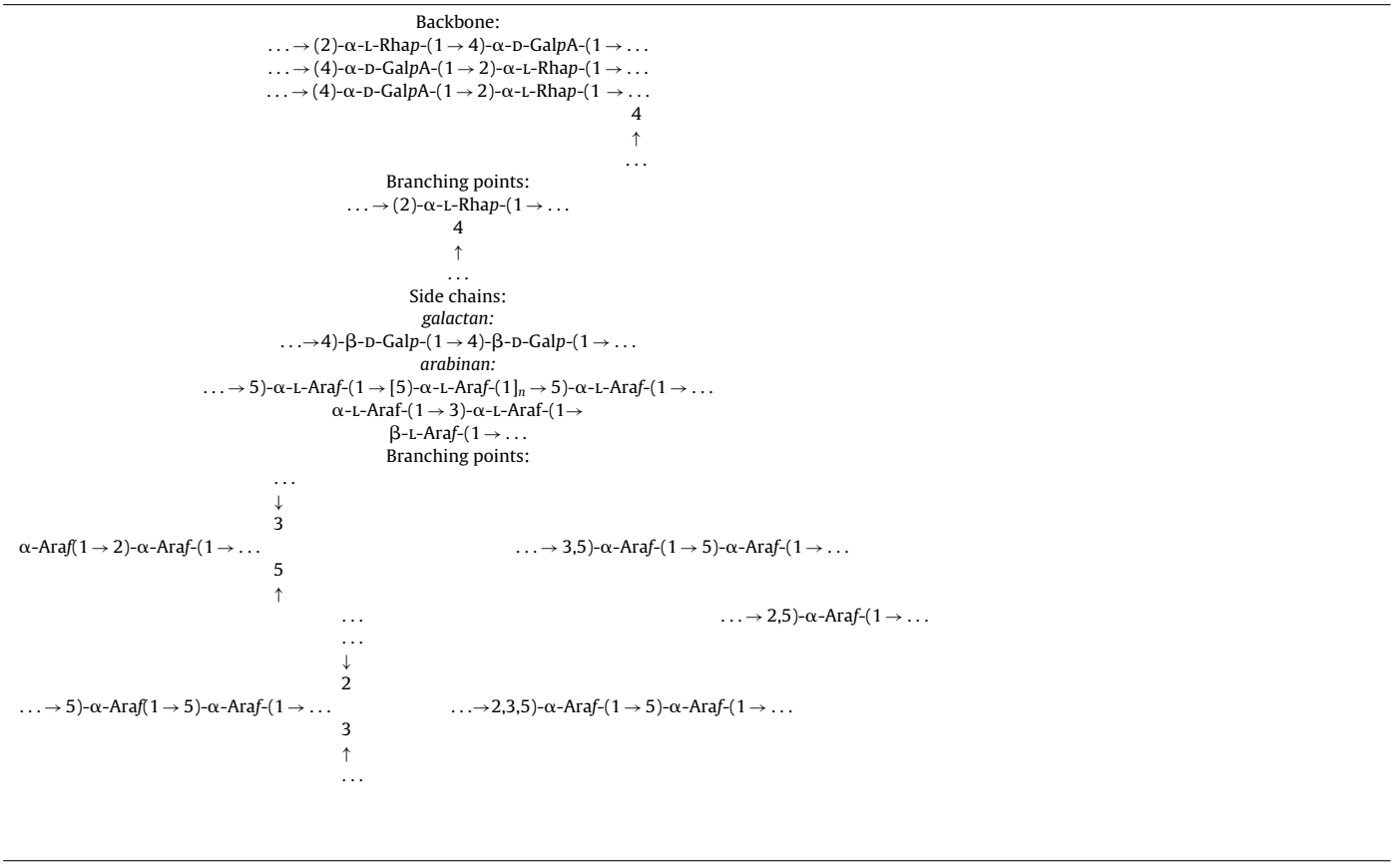

Acknowledgements

This work was performed in accordance with the research plan of the Institute of Chemistry, Komi Science Centre, Urals Branch of the Russian Academy of Sciences (IC KSC UB RAS) (2012–2014), and was partially supported from Joint Project of Basic Research no 12-C-3-1007 accomplished by IC KSC UB RAS in association with IPCET SB RAS. Simulation of the NMR spectra was powered by Carbohydrate Structure Database supported by Russian Foundation for Basic Research grant 12-04-00324. The authors thank S.P. Kuznetsov for recording of the NMR spectra, and F.V. Vityazev for molecular mass measurement (Institute of Chemistry, and Institute of physiology, respectively; Komi SC, Russian Academy of Sciences)

Appendix A. Supplementary data

Supplementary data associated with this article can be found, in the online version, at http://dx.doi.org/10.1016/j.carbpol.2014.07.037.

References

Albersheim, P., Darvill, A. G., O'Neill, M. A., Schols, H. A., & Voragen, A. G. J. (1996). A hypothesis: The same six polysaccharides are components of the primary cell walls of higher plants. In J. Visser, & A. G. J. Voragen (Eds.), *Pectins and pectinases* (pp. 47–55). Amsterdam: Elsevier Science.

Atmodjo, M. A., Hao, Z., & Mohnen, D. (2013). Evolving views of pectin biosynthesis. *Annual Review of Plant Biology*, *64*, 747–779.

Bradford, H. M. (1976). A rapid and sensitive method for the quantification of microgram quantities of protein utilizing the principal of protein-dye-binding. *Analytical Biochemistry*, *72*, 248–254.

Caffall, K. H., & Mohnen, D. (2009). The structure, function, and biosynthesis of plant cell wall pectic polysaccharides. *Carbohydrate Research*, *344*, 1879–1900.

Cardoso, S. M., Ferreira, J. A., Mafra, I., Silva, A. M. S., & Coimbra, M. A. (2007). Structural ripening-related changes of the arabinan-rich pectic polysaccharides from olive pulp cell walls. *Journal of Agricultural and Food Chemistry*, *55*, 7124–7130.

Coimbra, M. A., Cardoso, S. M., & Lopes-da-Silva, J. A. (2010). Olive pomace, a source for valuable arabinan-rich pectic polysaccharides. *Chemistry and Materials Science*, *294*, 129–141.

Cordeiro, L. M. C., de Fatima Reinhardt, V., Baggio, C. H., de Paula Werner, M. F., Burci, L. M., Sassaki, G. L., & Iacomini, M. (2012). Arabinan and arabinan-rich pectic polysaccharides from quinoa (*Chenopodium quinoa*) seeds: Structure and gastroprotective activity. *Food Chemistry*, *130*, 937–944.

Dourado, F., Cardoso, S. M., Silva, A. M. S., Gama, F. M., & Coimbra, M. A. (2006). NMR structural elucidation of the arabinan from *Prunus dulcis* immunobiological active pectic polysaccharides. *Carbohydrate Polymers*, *66*, 27–33.

Dubois, M., Gilles, K. A., Hamilton, J. K., Rebers, P. A., & Smith, F. (1956). Colorimetric method for determination of sugar sandrelated substances. *Analytical Chemistry*, *28*, 350–356.

Ele-Ekouna, J.-P., Pau-Roblot, C., Courtois, C., & Courtois, J. (2011). Chemical characterization of pectin from green tea (*Camellia sinensis*). *Carbohydrate Polymers*, *83*, 1232–1239.

El'kina, E. A., Shubakov, A. A., & Ovodov, Y. S. (2005). Vliyanie pektinov na rost zlakovyh kul'tur. *Himija rastitel'nogo syr'ja (Chemistry of plant raw material)*, *4*, 53–56.

Gorshkova, T. A. (2007). *Plant cell wall as dynamical system*. Moscow: Nauka (in Russian)

Habibi, Y., Mahrouz, M., & Vignon, M. R. (2005). Arabinan-rich polysaccharides isolated and characterized from the endosperm of the seed of *Opuntia ficusindica* prickly pear fruits. *Carbohydrate Polymers*, *60*, 319–329.

Harholt, J., Suttangkakul, A., & Scheller, H. V. (2010). Biosynthesis of pectin. *Plant Physiology*, *153*, 384–395.

Kim, H., & Ralph, J. (2010). Solution-state 2D NMR of ball-milled plant cell wall gels in DMSO-d6/pyridine-d5. *Organic & Biomolecular Chemistry*, *8*, 576–591.

Khodaei, N., & Karboune, S. (2013). Extraction and structural characterisation of rhamnogalacturonan I-type pectic polysaccharides from potato cell wall. *Food Chemistry*, *139*, 617–623.

Koffi, K. L., Yapo, B. M., & Besson, V. (2013). Extraction and characterization of gelling pectin from the peel of *Poncirus trifoliata* fruit. *Agricultural Sciences*, *4*, 614–619.

Leontein, K., & Lonngren, J. (1993). Determination of the absolute configuration of sugars by gas–liquid chromatography of their acetylated 2-octyl glycosides. *Methods in Carbohydrate Chemistry*, *9*, 87–89.

Lerouge, P., O'Neill, M. A., Darvill, A. G., & Albersheim, P. (1993). Structural characterization of endo-glycanase-generated oligoglycosyl side chains of rhamnogalacturonan-I. *Carbohydrate Research*, *243*, 359–371.

Makarova, E. N., Patova, O. A., Shakhmatov, E. G., Kuznetsov, S. P., & Ovodov, Y. S. (2013). Structural studies of the pectic polysaccharide from Siberian fir (*Abies sibirica* Ledeb.). *Carbohydrate Polymers*, *92*, 1817–1826.

Mandal, S., Patra, S., Dey, B., Bhunia, S. K., Maity, K. K., & Islam, S. S. (2011). Structural analysis of an arabinan isolated from alkaline extract of the endosperm of seeds of *C. bonduc* (Nata Karanja). *Carbohydrate Polymers*, *84*, 471–476.

Mikshina, P. V., Gurjanov, O. P., Mukhitova, F. K., Petrova, A. A., Shashkov, A. S., & Gorshkova, T. A. (2012). Structural details of pectic galactan from the secondary cell walls of flax (*Linum usitatissimum* L.) phloem fibres. *Carbohydrate Polymers*, *87*, 853–861.

M'sakni, N. H., Majdoub, H., Roudesli, S., Picton, L., Le Cerf, D., Rihouey, C., & Morvan, C. (2006). Composition, structure and solution properties of polysaccharides extracted from leaves of *Mesembryanthenum crystallinum*. *European Polymer Journal*, *42*, 786–795.

Naran, R., Chen, G., & Carpita, N. C. (2008). Novel rhamnogalacturonan-I and arabinoxylan polysaccharides of flax seed mucilage. *Plant Physiology*, *148*, 132–141.

Navarro, D. A., Cerezo, A. S., & Stortz, C. A. (2002). NMR spectroscopy and chemical studies of an arabinan-rich system from the endosperm of the seed of *Gleditsia triacanthos*. *Carbohydrate Research*, *337*, 255–263.

Nie, S. P., Wang, C., Cui, S. W., Wang, Q., Xie, M. Y., & Phillips, G. O. (2013). A further amendment to the classical core structure of gum arabic (*Acacia senegal*). *Food Hydrocolloids*, *31*, 42–48.

Oosterveld, A., Beldman, G., Schols, H. A., & Voragen, A. G. J. (2000). Characterization of arabinose and ferulic acid rich pectic polysaccharides and hemicelluloses from sugar beet pulp. *Carbohydrate Research*, *328*, 185–197.

Ovodov, Y. S. (2009). Current views on pectin substances. *Russian Journal of Bioorganic Chemistry*, *35*(3), 269–284.

Perrone, P., Hewage, C. M., Thomson, A. R., Bailey, K., Sadler, I. H., & Fry, S. C. (2002). Patterns of methyl and *O*-acetyl esterification in spinach pectins: New complexity. *Phytochemistry*, *60*, 67–77.

Petersen, B. O., Meier, S., Duus, J. Ø., & Clausen, M. H. (2008). Structural characterization of homogalacturonan by NMR spectroscopy-assignment of reference compounds. *Carbohydrate Research*, *343*, 2830–2833.

Redgwell, R. J., Curti, D., Wang, J., Dobruchowska, J. M., Gerwig, G. J., Kamerling, J. P., & Bucheli, P. (2011). Cell wall polysaccharides of Chinese Wolfberry (*Lycium barbarum*): Part 2: Characterisation of arabinogalactan-proteins. *Carbohydrate Polymers*, *84*, 1075–1083.

Ridley, B. L., O'Neill, M. A., & Mohnen, D. A. (2001). Pectins: Structure, biosynthesis, and oligogalacturonide-related signaling. *Phytochemistry*, *57*, 929–967.

Simkovic, I., Uhliariková, I., Yadav, M. P., & Mendichi, R. (2010). Branched arabinan obtained from sugar beet pulp by quaternization under acidic conditions. *Carbohydrate Polymers*, *82*, 815–821.

Schols, H. A., Posthumus, M. A., & Voragen, A. G. J. (1990). Hairy (ramified) regions of pectins. 1. Structural features of hairy regions of pectins isolated from apple juice produced by the liquefaction process. *Carbohydrate Research*, *206*, 117–129.

Shakhmatov, E. G., Toukach, P. V., Kuznetsov, S. P., & Makarova, E. N. (2014). Structural characteristics of water-soluble polysaccharides from *Heracleum sosnowskyi* Manden. *Carbohydrate Polymers*, *102*, 521–528.

Steinhorn, G., Sims, I. M., Carnachan, S. M., Carr, A. J., & Schlothauer, R. (2011). Isolation and characterisation of arabinogalactan-proteins from New Zealand kanuka honey. *Food Chemistry*, *128*(4), 949–956.

Swamy, N. R., & Salimath, P. V. (1991). Arabinans from *Cajanus cajan* cotyledon. *Phytochemistry*, *30*, 263–265.

Taboada, E., Fisher, P., Jara, R., Zúniga, E., Gidekel, M., Cabrera, J. C., Pereirag, E., Gutiérrez-Moragah, A., Villalongai, R., & Cabrera, G. (2010). Isolation and characterisation of pectic substances from murta (*Ugni molinae* Turcz) fruits. *Food Chemistry*, *123*, 669–678.

Toukach, F. V., & Ananikov, V. P. (2013). Recent advances in computational predictions of NMR parameters for structure elucidation of carbohydrates: Methods and limitations. *Chemical Society Reviews*, *42*, 8376–8415.

Thude, S., & Classen, B. (2005). High molecular weight constituents from roots of Echinacea pallida: An arabinogalactan-protein and an arabinan. *Phytochemistry*, *66*, 1026–1032.

Usov, A. I., Bilan, M. I., & Klochkova, N. G. (1995). Polysaccharide of algae 48. Polysaccharide composition of several calcareous red algae: Isolation of alginate from *Corallina pilutitara* P. et R. (*Rhodophyta Corallinaceae*). *Botanica Marina*, *38*, 43–51.

Westphal, Y., Kühnel, S., Waard, P., Hinz, S. W. A., Schols, H. A., Voragen, A. G. J., & Gruppen, H. (2010). Branched arabino-oligosaccharides isolated from sugar beet arabinan. *Carbohydrate Research*, *345*, 1180–1189.

Willfor, S., Sjoholm, R., Laine, C., & Holmbom, B. (2002). Structural features of water-soluble arabinogalactans from Norway spruce and Scots pine heartwood. *Wood Science and Technology*, *36*, 101–110.

Wood, P. J., & Siddiqui, I. R. (1971). Determination of methanol and its application to measurement of pectin ester content and pectin methyl esterase activity. *Analytical Biochemistry*, *39*, 418–423.

Yapo, B. M. (2011). Rhamnogalacturonan—I: A structurally puzzling and functionally versatile polysaccharide from plant cell walls and mucilages. *Polymer Reviews*, *51*(4), 391–413.

York, W. S., Darvill, A. G., McNeil, M., Stevenson, T. T., & Albersheim, P. (1985). Isolation and characterization of plant cell walls and cell-wall components. *Methods of Enzymology*, *118*, 3–40.

Zheng, Y., & Mort, A. (2008). Isolation and structural characterization of a novel oligosaccharide from the rhamnogalacturonan of *Gossypium hirsutum* L. *Carbohydrate Research*, *343*, 1041–1049.